

One-pot Syntheses of Metallic Hollow Nanoparticles of Tin and Lead

Gaehang Lee,^{†‡} Sang-Il Choi,^{*} Young Hwan Lee,[†] and Joon T. Park^{†*}

[†]Department of Chemistry and School of Molecular Science (BK 21), Korea Advanced Institute of Science and Technology (KAIST), Daejeon 305-701, Korea. *E-mail: joontpark@kaist.ac.kr.

[‡]Division of Materials Science, Korea Basic Science Institute (KBSI), Daejeon 305-333, Korea

Received December 2, 2008. Accepted March 27, 2009

Hollow Sn and Pb nanoparticles have been prepared by a rapid injection of an aqueous solution of SnCl₂-poly(vinylpyrrolidone) (PVP, surfactant) and Pb(OAc)₂·3H₂O-PVP into an aqueous solution of sodium borohydride (reducing agent) in simple, one-pot reaction at room temperature under an argon atmosphere, respectively. The two hollow nanoparticles have been fully characterized by TEM, HRTEM, SAED, XRD, and EDX analyses. Upon exposure to air, the black Pb hollow nanoparticles are gradually transformed into a mixture of Pb, litharge (tetragonal PbO), massicot (orthorhombic PbO), and Pb₃O₈. The order and speed of mixing of the reactants between the metal precursor-PVP and the reductant solutions and stoichiometry of all the reactants are crucial factors for the formation of the two hollow nanocrystals. The Sn and Pb hollow nanoparticles were produced only when 1:(1.5-2) and 1:3 ratios of the Sn and Pb precursors to NaBH₄ were employed with a rapid injection, respectively.

Key Words: Hollow, PVP, NaBH₄, Tin, Lead

Introduction

Nanostructures with an empty core are fascinating materials due to several advantages such as low density, high surface area, lighter weight, and reduced cost compared to their solid counterparts. In particular, hollow nanomaterials exhibit superior characteristics in their applications such as catalysis,¹ fuel cell,²⁻³ biotechnology,⁴⁻⁶ lubricant,⁷ and nanoreactor.⁸ Metallic hollow nanoparticles have been prepared from the general synthetic strategy that the surface of templates (e.g., silver,⁹⁻¹² selenium,¹³ cobalt,^{21,14} polymer latex,^{15,16} and silica^{1,17-19}) is covered by desired metals, and then the core templates were selectively removed through calcination, wet chemical etching, and galvanic replacement. Great challenges still remain, however, in preparing hollow spheres *via* one-step thermal solution reactions.

Tin nanostructures have been shown to exhibit a high catalytic activity in the dehydrogenation of isobutene,²⁰ and enhanced capacity and cycling stability when alloyed with lithium for secondary battery applications.²¹ Tin nanoparticles have been prepared through the methods of thermal evaporation of a bulk tin ball,²² reaction of SnCl₄, Mg₂Sn, and *n*-C₄H₉Li in ethylene glycol dimethyl ether,²³ and reduction of SnCl₄·5H₂O by tetraoctylammonium bromide in dichloromethane.²¹ Lead nanostructures are attractive materials for its potential applications in superconductor²⁴ and photonic crystal.²⁵ Lead nanoparticles have been prepared by reduction of Pb[N(SiMe₃)₂]₂ by H₂Al(O^{*i*}Bu)²⁶ and polyol reduction of Pb(CH₃COO)₂·3H₂O.²⁵

Herein we report simple, one-pot syntheses of hollow Sn and Pb nanoparticles by employing SnCl₂ or Pb(OAc)₂·3H₂O (Ac = CH₃CO) as a precursor, sodium borohydride as a reducing agent, and poly(vinylpyrrolidone) (PVP) as a surfactant under extremely mild conditions at room temperature.

Experimental Section

All reactions were carried out under an argon atmosphere with use of standard Schlenk techniques. Ultra-pure water was obtained from Milli-Q immediately before use. SnCl₂ (98%, Strem Chemicals), Pb(OAc)₂·3H₂O (99%, Yakuri Pure Chemicals), poly(vinylpyrrolidone) (PVP, M_w ≈ 55,000 Dalton, Sigma-Aldrich), sodium borohydride (98%, Aldrich), and 1-methyl-2-pyrrolidone (99%, Aldrich) were used without further purification.

The hollow Sn nanoparticles (10 ± 1.4 nm in diameter with a 5 ± 0.9 nm hole) were prepared by a rapid injection of a mixture of SnCl₂ (50 mg) and poly(vinyl pyrrolidone) (PVP) (295 mg, M_w = 55,000) in ultra-pure H₂O (2 mL) into an aqueous NaBH₄ (10 mg) solution (H₂O, 8 mL) under an argon atmosphere at room temperature. The reaction was allowed to proceed for 10 min. To the resulting reaction mixture was added ethanol (20 mL) and centrifuged at 14,000 rpm for 30 min to remove byproducts and excess PVP. Similar repeated purification (3 times) with ethanol (20 mL) gave a black precipitate, which could be readily re-dispersed in various hydrophilic solvents such as methanol, ethanol, and water. The hollow Pb nanocrystals (51 ± 7 nm in diameter with a 30 ± 4 nm hole) were similarly prepared by the procedure described above for the preparation of the hollow Sn nanoparticles except that Pb(OAc)₂·3H₂O (70 mg), PVP (205 mg), and NaBH₄ (10.5 mg) were used.

The Sn, Pb, and composite (Pb, litharge (PbO), massicot (PbO), and Pb₃O₈) hollow nanocrystals were characterized by XRD (Rigaku D/MAX-RB (12 kW) diffractometer using graphite-monochromatized Cu-Kα radiation at 40 kV and 45 mA and Bruker D8 Advance (3 kW) with Vantec detector diffractometer using Ge (111)-Cu Kα1 radiation at 50 kV and 40 mA), TEM (low resolution: Omega EM912 operated at 120 kV; high resolution: Philips F20Tecnai operated at 200

kV; EDX line analysis: Tecnai G2 F30 S-TWIN operated at 300 kV), and selected area electron diffraction (SAED) patterns attached to EM912. Samples for TEM investigations were prepared by placing an aliquot of ethanol solution onto an amorphous carbon substrate supported on a copper grid and allowing the grid to dry at room temperature.

Results and Discussion

Hollow Sn and Pb nanoparticles have been prepared by a rapid injection of an aqueous solution of SnCl_2 -poly(vinylpyrrolidone) (PVP, surfactant) and $\text{Pb}(\text{OAc})_2 \cdot 3\text{H}_2\text{O}$ -PVP into an aqueous solution of sodium borohydride (reducing agent) in one-pot reaction at room temperature under an argon atmosphere, respectively. The evidence for the hollow nature of nanocrystalline Sn and Pb is seen in the TEM and EDX analyses of the materials. Both TEM (Figure 1) and HRTEM (the insets) images of Sn or Pb nanoparticles reveal that the middle part is brighter than the edge of the particles, clearly indicating a well-defined void. The hollow Sn nanoparticles tend to be collapsed by the e-beam during the TEM measurement (Figure S1 in the supporting information). Furthermore, Figure 2 shows the EDX line analysis across a single Pb particle (Tecnai G2 F30 S-TWIN operated at 300 kV, 60 pixel size, and 3 sec dwell time). The Pb L line decreases from the outer wall toward the center. We were not able to obtain a well-defined Sn line analysis, because the Sn nanostructure

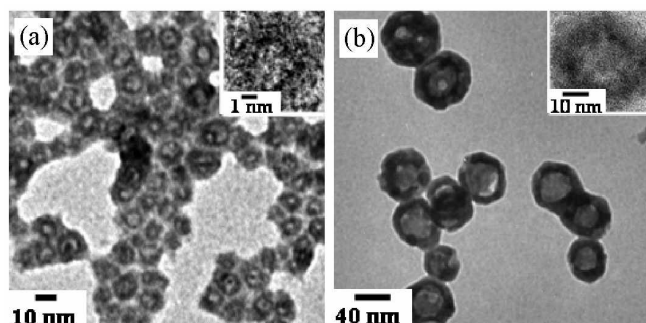


Figure 1. TEM images of hollow (a) Sn and (b) Pb nanoparticles. (inset: HRTEM images of a single hollow (a) Sn and (b) Pb nanoparticle.)

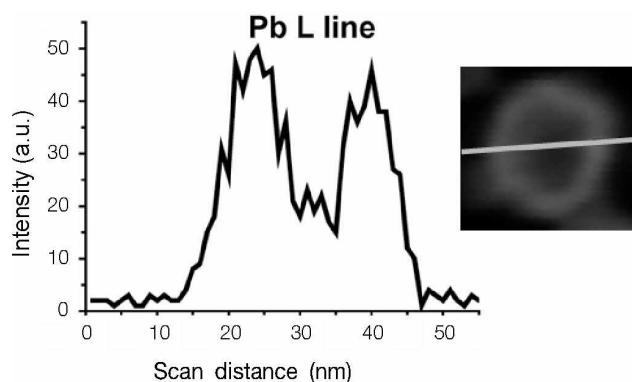


Figure 2. The EDX line analysis across a single hollow Pb nanoparticle (dark-field TEM image of ca. 38 nm nanoparticle).

collapsed when exposed to the e-beam of the TEM as indicated above. The XRD data (Figure 3) of the hollow Sn and Pb nanoparticles are consistent with a tetragonal structure for Sn (JCPDS card No. 65-2631) and a cubic structure for Pb (JCPDS card No. 65-2873). The SAED pattern of the hollow Sn nanoparticles in Figure 4(a) matches well with the XRD data of this material.

The following results render some insight into this novel phenomena of the formation of the hollow nanoparticles. The hollow nanoparticles form only in very limited ranges of stoichiometric ratios of the precursor, surfactant, and reducing agent, as indicated in the synthetic procedures. The hollow nanoparticles are formed in the early stage of the reactions within a few minutes. The Pb hollow nanoparticles were produced only when a 1:3 ratio of the Pb precursor to NaBH_4 was employed with a rapid injection. Upon exposure to air, the color of the solution containing black Pb hollow nanoparticles gradually changed from black to pale yellow. The SAED (Figure 4(b)), XRD (Figure S3), and HRTEM (Figure S4) data of these pale yellow particles indicated that a mixture of Pb, litharge (tetragonal PbO), massicot (orthorhombic PbO), and Pb_3O_8 formed. When a $\text{Pb}(\text{OAc})_2 \cdot 3\text{H}_2\text{O}$ aqueous solution instead of a $\text{Pb}(\text{OAc})_2 \cdot 3\text{H}_2\text{O}$ -PVP solution was added to an aqueous solution of NaBH_4 and PVP, only solid nanoparticles (5 ± 1.8 nm) were formed, and their hollow counterparts were not observed.

In the case of Sn nanocrystal formation, a dropwise addition of an aqueous mixture of SnCl_2 and PVP to an aqueous solution of NaBH_4 resulted in the formation of mixed nanoparticles with solid 11 ± 1.7 nm (89%) and hollow 9 ± 1.6 nm with a 5 ± 0.8 nm hole (11%) (Figure S5(a)). If reagents are added in a dropwise and reverse way, this also led to mixed nanoparticles

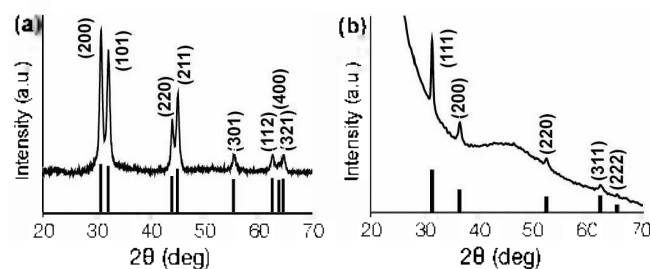


Figure 3. XRD patterns of hollow (a) Sn and (b) Pb nanoparticles in a PMMA sample holder (Figure S2). The standard peaks from the JCPDS cards are shown as bar diagrams at the bottom.

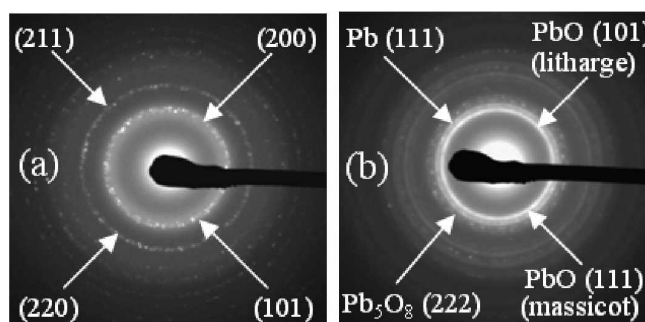


Figure 4. SAED patterns of hollow (a) Sn and (b) Pb nanoparticles.

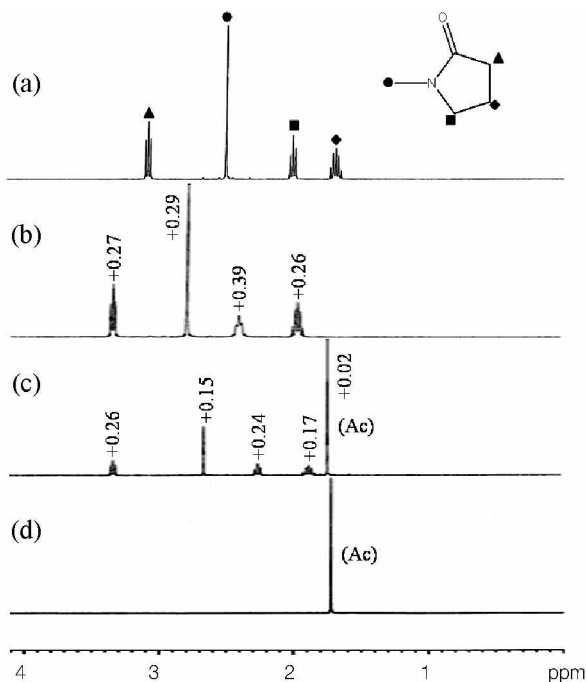


Figure 5. ^1H NMR spectra of (a) 1-methyl-2-pyrrolidone (mpy), (b) $\text{SnCl}_2\cdot\text{mpy}$, (c) $\text{Pb}(\text{OAc})_2\cdot 3\text{H}_2\text{O}\cdot\text{mpy}$, and (d) $\text{Pb}(\text{OAc})_2\cdot 3\text{H}_2\text{O}$. Numbers provided in (b) and (c) are relative chemical shift differences from values for pure mpy and $\text{Pb}(\text{OAc})_2\cdot 3\text{H}_2\text{O}$, respectively.

of solid 10 ± 1.5 nm (63%) and hollow 9 ± 1.1 nm with a 5 ± 0.6 nm hole (37%) (Figure S5(b)). However, in a rapid injection of $\text{SnCl}_2\text{-PVP}$ to NaBH_4 , the shape of hollow nanoparticles was strongly dependent on the stoichiometric NaBH_4 to Sn precursor ratio. With (i) 1, (ii) 1.5, (iii) 2, and (iv) 3 equivalent ratios of NaBH_4 to Sn, (i) solid 9 ± 0.7 nm, (ii) hollow 9 ± 1.1 nm with a 2 ± 0.9 nm hole, (iii) hollow 10 ± 1.4 nm with a 5 ± 0.9 nm hole, and (iv) solid 11 ± 1.5 nm (87%) and hollow 9 ± 0.7 nm with a 3 ± 1.1 nm hole (13%) of Sn particles, were produced, respectively (Figure S6). Hollow Sn particles were only formed with a 1:(1.5-2) ratio of the Sn precursor to NaBH_4 . These results imply that the interaction between metal precursors and PVP as well as rapid reduction of metal precursors are the critical factors for the production of hollow structures.

The PVP surfactant is the only one that yields the hollow nanoparticles among various surfactants tested such as cetyltrimethylammonium bromide, poly(propylene carbonate), and polyacrylamide. The insoluble SnCl_2 precursor in water becomes soluble upon mixing with the PVP ligand, implying that Sn^{2+} (Pb^{2+} in the other case) strongly interacts with PVP as previously reported.²⁷ The ^1H NMR spectra of an aqueous solution of SnCl_2 and 1-methyl-2-pyrrolidone (mpy) and that of $\text{Pb}(\text{OAc})_2\cdot 3\text{H}_2\text{O}$ and mpy reveal *av.* 0.30 and 0.21 ppm downfield shifts compared to the pure mpy peaks, respectively, as shown in Figure 5. The mpy was employed instead of PVP in order to observe sharp NMR signals. The $\text{Sn}^{2+}\text{-PVP}$ and $\text{Pb}^{2+}\text{-PVP}$ interactions exhibit a red shift of PVP $\nu(\text{CO})$ of 69.9 cm^{-1} and 4.7 cm^{-1} relative to PVP, respectively, in the IR spectra (Figure S7). The $\text{Pb}^{2+}\text{-PVP}$ interaction shows a blue shift of the acetate $\nu(\text{CO})$ of *av.* 2.9 cm^{-1} relative to the pure

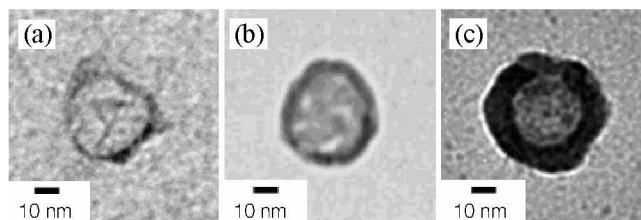


Figure 6. Size growth of hollow Pb nanoparticles: (a) 43 nm with a shell thickness of 1.7 nm immediately after injection, (b) 44 nm with a 4.5 nm shell thickness after 1 min, (c) 56 nm with a 11 nm shell thickness after 10 min.

$\text{Pb}(\text{OAc})_2\cdot 3\text{H}_2\text{O}$. These results suggest that the interaction of SnCl_2 with PVP is stronger than that of $\text{Pb}(\text{OAc})_2\cdot 3\text{H}_2\text{O}$ with PVP. Tin ion with smaller chloride ligands is, presumably, more open to the PVP coordination than lead ion with larger acetate ligands. The interactions of Sn and Pb nanoparticles with PVP reveal a red shift of PVP $\nu(\text{CO})$ of 11.2 cm^{-1} and 19.8 cm^{-1} relative to PVP, respectively. In comparison, a red shift of the PVP carbonyl frequency of *ca.* 60 cm^{-1} has been reported due to the strong $\text{C}=\text{O}\rightarrow\text{Pt}$ interaction for Pt nanoparticles capped with the PVP surfactant.²⁸

The TEM image of the sample taken immediately after injection of $\text{Pb}(\text{OAc})_2\cdot 3\text{H}_2\text{O}\text{-PVP}$ solution into a NaBH_4 solution showed hollow nanoparticles of 43 nm with a thin shell thickness of 1.7 nm (Figure 6(a)), and the size evolution was observed as the reaction proceeds [44 nm with a 4.5 nm shell thickness after 1 min (Figure 6(b)) and 56 nm with a 11 nm shell thickness after 10 min (Figure 6(c))]. Proposing detailed pathways for the formation of hollow nanoparticles from our data provided in this work is unfeasible, but it is likely that the reduction of metal ions bound on PVP form a thin metallic hollow nanostructures and subsequent growth of this shape occurs from both sides of the shell by further reduction of metal ions in the bulk water and those in the inside of the hollow nanocrystals as observed in Figure 6. The fast nucleation and growth processes seem to be important factors for the formation of hollow nanoparticles, since an instantaneous reduction of metal ions took place in the presence of large excess of the reducing agent in comparison to the metal precursors.

The syntheses of hollow metallic nanoparticles are limited to a few approaches. The most common methods involve the deposition of metal onto solid nano-template metal, silica and other materials and subsequent removal of the templating core by dissolution or calcination, and the galvanic replacement reactions. The coassembly of metallic nanoparticles with organic molecules have been employed to construct hollow nanospheres.²⁹ An interesting method for making hollow Pt nanoparticles using templating liposomes containing photocatalyst molecules has been recently reported.³⁰ Hollow Gold nanocubes have also been prepared by electron beam reduction.³¹ Our method is a unique, novel, and important addition to the syntheses of hollow metallic nanoparticles.

Conclusion

The first synthetic examples of hollow Sn and Pb nano-

structures have been shown in aqueous solution and at room temperature by one-step synthetic methods. The order and speed of mixing of the reactants between the metal precursor-PVP and the reductant solutions and stoichiometry of all the reactants are crucial factors for the formation of the hollow nanocrystals. The hollow lead nanoparticles are so reactive that it could be used for making other hollow, inorganic, and derivatized, lead nanomaterials. We anticipate our approach will provide new opportunities in the preparation of varieties of hollow nanoparticles by simple, one-pot synthetic reactions. We are currently investigating the generality of our method for the preparation of metallic hollow nanoparticles.

Supporting Information Available. Synthetic procedures, XRD data of composite hollow Pb nanocrystals and the sample holder, TEM images and SAED patterns of Sn and Pb nanoparticles, ^1H NMR spectra of mpy, $\text{SnCl}_2\text{-mpy}$, $\text{Pb}(\text{OAc})_2\cdot 3\text{H}_2\text{O}\text{-mpy}$, and $\text{Pb}(\text{OAc})_2\cdot 3\text{H}_2\text{O}$, and IR spectra of PVP, $\text{Pb}(\text{OAc})_2\cdot 3\text{H}_2\text{O}$, $\text{SnCl}_2\text{-PVP}$, $\text{Pb}(\text{OAc})_2\cdot 3\text{H}_2\text{O}\text{-PVP}$, Sn nanoparticle-PVP, and Pb nanoparticle-PVP.

Acknowledgments. This work was supported by the Korea Research Foundation Grant funded by the Korean Government (MOEHRD; KRF-2005-201-C00021) and by the Nano R&D program (Grant 2005-02618) of the Korea Science and Engineering Foundation (KOSEF) funded by the Korean Ministry of Science & Technology (MOST). This work was also supported in part by the SRC program (Grant R11-2005-008-00000-0) of the KOSEF through the Center for Intelligent Nano-Bio Materials at Ewha Woman's University. We thank the staff of KBSI and KAIST for assistance with TEM analyses and Dr. S.-T. Hong of LG Chem, Ltd. for XRD analyses. Prof. D. G. Churchill of KAIST is acknowledged for his proofreading of this manuscript.

References.

- Kim, S.-W.; Kim, M.; Lee, W. Y.; Hyeon, T. *J. Am. Chem. Soc.* **2002**, *124*, 7642.
- Liang, H.-P.; Zhang, H.-M.; Hu, J.-S.; Guo, Y.-G.; Wan, L.-J.; Bai, C.-L. *Angew. Chem. Int. Ed.* **2004**, *43*, 1540.
- Yang, J.; Lee, J. Y.; Too, H.-P.; Valiyaveetil, S. J. *Phys. Chem. B* **2006**, *110*, 125.
- Mathiowitz, E.; Jacob, J. S.; Jon, Y. S.; Carino, G. P.; Chickering, D. E.; Chaturvedi, P.; Santos, C. A.; Vijayaraghavan, K.; Montgomery, S.; Bassett, M.; Morrell, C. *Nature* **1997**, *386*, 410.
- Son, S. J.; Reichel, J.; He, B.; Schuchman, M.; Lee, S. B. *J. Am. Chem. Soc.* **2005**, *127*, 7316.
- Im, S. H.; Jeong, U.; Xia, Y. *Nature Mater.* **2005**, *4*, 671.
- Rapoport, L.; Bilik, Yu.; Feldman, Y.; Homyonfer, M.; Cohen, S. R.; Tenne, R. *Nature* **1997**, *387*, 791.
- Yin, Y.; Rioux, R. N.; Erdonmez, C. K.; Hughes, S.; Somorjai, G. A.; Alivisatos, A. P. *Science* **2004**, *304*, 711.
- Sun, Y.; Mayers, B.; Xia, Y. *Adv. Mater.* **2003**, *15*, 641.
- Yin, Y.; Erdonmez, C.; Aloni, S.; Alivisatos, A. P. *J. Am. Chem. Soc.* **2006**, *128*, 2671.
- Sun, Y.; Mayers, B.; Xia, Y. *Nano Lett.* **2002**, *2*, 481.
- Kim, S. J.; Ah, C. S.; Jang, D.-J. *Adv. Mater.* **2007**, *19*, 1064.
- Mayers, B.; Jiang, X.; Sunderland, D.; Cattle, B.; Xia, Y. *J. Am. Chem. Soc.* **2003**, *125*, 13364.
- Liang, H.-P.; Guo, Y.-G.; Zhang, H.-M.; Hu, J.-S.; Wan, L.-J.; Bai, C.-L. *Chem. Comm.* **2004**, *13*, 1496.
- Breen, M. L.; Dinsmore, A. D.; Pink, R. H.; Qadri, S. B.; Ratna, B. R. *Langmuir* **2001**, *17*, 903.
- Liang, Z. J.; Susha, A.; Caruso, F. *Chem. Mater.* **2003**, *15*, 3176.
- Jiang, P.; Bertone, J. F.; Colvin, V. L. *Science* **2001**, *291*, 453.
- Prodan, E.; Radloff, C.; Halas, N. J.; Nordlander, P. *Science* **2003**, *302*, 419.
- Lu, L. H.; Capek, R.; Kornowski, A.; Gaponik, N.; Eychmuller, A. *Angew. Chem. Int. Ed.* **2005**, *44*, 5997.
- Casella, M. L.; Siri, G. J.; Santori, G. F.; Ferretti, O. A. *Langmuir* **2000**, *16*, 5639.
- Noh, M.; Kim, Y.; Kim, M. G.; Lee, H.; Kim, H.; Kwon, Y.; Lee, Y.; Cho, J. *Chem. Mater.* **2005**, *17*, 3320.
- Hsu, Y. J.; Lu, S.-Y.; Lin, Y.-F. *Small* **2006**, *2*, 26.
- Yang, C.-S.; Liu, Y. Q.; Kauzlarich, S. M. *Chem. Mater.* **2000**, *12*, 983.
- Kittel, C. *Introduction to Solid State Physics*; John Wiley & Sons: New York, 1996.
- Wang, Y.; Xia, Y. *Nano Lett.* **2004**, *4*, 2047.
- Veith, M.; Frères, J.; König, P.; Schütt, O.; Huch, V.; Blin, J. *Eur. J. Inorg. Chem.* **2005**, 3699.
- Vasquez, Y.; Sra, A. K.; Schaak, R. E. *J. Am. Chem. Soc.* **2005**, *127*, 12504.
- Borodko, Y.; Habas, S. E.; Koebel, M.; Yang, P.; Frei, H.; Somorjai, G. A. *J. Phys. Chem. B* **2006**, *110*, 23052.
- Wong, M. S.; Cha, J. N.; Choi, K.-S.; Deming, T. J.; Stucky, G. D. *Nano Lett.* **2002**, *2*, 583.
- Song, Y.; Garcia, R. M.; Dorin, R. M.; Wang, H.; Qiu, Y.; Shelnutt, J. A. *Angew. Chem. Int. Ed.* **2006**, *45*, 8126.
- Halder, A.; Ravishankar, N. *J. Phys. Chem. B* **2006**, *110*, 6595.